Bird's-eye view of an Ediacaran subglacial landscape

Daniel Paul Le Heron[1*†], Thomas Matthew Vandyk[2], Hongwei Kuang[3*], Yongqing Liu[3†], Xiaoshuai Chen[3], Yuchong Wang[3], Zhenrui Yang[3], Lars Scharfenberg[1], Bethan Davies[2], and Graham Shields[4]

[1]Department of Geodynamics and Sedimentology, University of Vienna, Althanstrasse 14, A-1090 Vienna, Austria
[2]Department of Geography, Royal Holloway University of London, Surrey TW20 0EX, UK
[3]Institute of Geology, Chinese Academy of Geological Sciences, No. 26 Baiwanzhuang Street, 100037 Beijing, China
[4]Department of Earth Sciences, University College London, Gower Street, London WC1E 6BT, UK

ABSTRACT

Depositional evidence for glaciation (dropstones, diamictites) is common in Neoproterozoic strata, and often debated, but erosional evidence (e.g., unconformities cut directly by ice) is rare. Only two such unconformities are known to have been well preserved globally from the Ediacaran Period (in western Australia and central China). This paper provides the first full description of a spectacular subglacial landscape carved beneath ice masses in the Shimengou area of central China, with classical subglacial bed forms including general faceted forms, müschelbruche, cavetto, spindle forms, and striations that testify to an abundance of meltwater during subglacial erosion. These features were produced during the southward, somewhat sinuous, flow of a temperate to polythermal ice mass.

INTRODUCTION

Ediacaran glaciation (ca. 635–541 Ma) is reported from multiple ancient landmasses (Amazonia, Australia, Avalonia, Baltica, Laurentia, North China, and Tarim cratons; Li et al., 2013). In these strata, most evidence for glaciation is depositional, either via ice-rafted debris or background sedimentation (Spence et al., 2016, their figure 2) or indirectly as sediment gravity flows of possible glacial origin (Carto and Eyles, 2012). Erosional evidence in the form of subglacial landforms is rare. Globally, the outcrop situation (steeply dipping or folded rocks, little extensive bedding plane exposure) may be a prime reason for this, together with weathering of the patina that typically preserves striations (Siman-Tov et al., 2017). Striated pavements have poor preservation potential (Montes et al., 1985; see Laajoki, 2002, his table 3). Most Precambrian examples are meter-scale fragments (Mirams, 1964; Lu and Gao, 1994; Rice and Hoffman, 2000; Etienne et al., 2011; Etemad-Saeed et al., 2016), and the glacial interpretation of others is challenged (Crowell, 1964; Daily et al., 1973; Christie-Blick, 1982; Jensen and Wulff-Pedersen, 1996).

The striated pavements of the Luoquan Formation, North China craton (Fig. 1), are

(1) world-class in areal extent and the quality of fine detail that they preserve, and (2) one of only two surviving sets of Ediacaran age known globally. The only comparable example is from Western Australia, where several surfaces have been interpreted beneath the Egan Formation, but only briefly described in general terms (Perry and Roberts, 1968; Corkeron and George, 2001; Corkeron, 2011). Despite being known for over 30 yr, the Luoquan pavements have been subject to only basic description (Mu, 1981; Guan et al., 1986; Wu and Guan, 1988). Indeed, this level of description applies to all known Precambrian subglacial surfaces, contrasting with the abundance of data available for recent subglacial bedrock surfaces from the smallest (Iverson, 1991) to the largest (Krabbendam et al., 2016) scales. Addressing this, we present new drone-acquired photogrammetry and digital terrain models, supported by conventional field observations, detailing the most spectacular of the Luoquan Formation pavements from the Shimengou area of Henan Province, China. This is the first time that a pre-Pleistocene subglacially striated surface has been recorded and mapped using these aerial techniques or in such a level of detail.

GEOLOGIC SETTING

During the Neoproterozoic Era, the Shimengou area near Pingdingshan (Fig. 1) was part of the North China block, over which ice masses extended to deposit the Luoquan For-
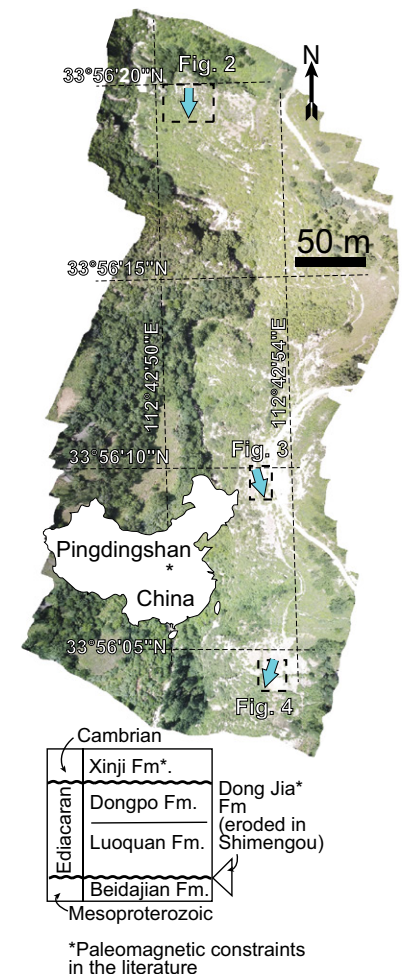
Figure 1. Aerial photograph of Shimengou pavement (near Pingdingshan City) in central China showing simplified striation orientations and interpreted ice flow (arrows) in three main study areas (north, central, south) described in text. Note coordinates enabling reader to find study area. Stratigraphic column also highlights intervals with paleomagnetic constraint: the Dong Jia Formation (Huang et al., 1999; Zhang et al., 2000) and the Xinji Formation (Fu et al., 2015).

mation. This formation and correlative glaciogenic units (e.g., Fengtai, Zhengmuguan, Hongtiegou Formations) are intermittently exposed over ~2000 km across the Central China orogen. Establishment of ice-contact lake systems during deposition of the Luoquan Formation (Guan et al., 1986) is envisaged, with vertical gradations between dropstone-bearing shales, stratified diamictites, and massive diamictites interpreted as waterlain deposits rather than tillites (Le Heron et al., 2018). Uppermost Ediacaran fossils from apparently conformable, overlying nonglacial units strongly suggest a late Ediacaran age (ca. 550 Ma) for the Luoquan glaciation (Shen et al., 2007; Zhou et al., 2018). Low paleolatitudes for the North China block during the late Ediacaran and Cambrian are interpreted (Li et al., 2013; Merdith et al., 2017), although the Luoquan Formation lacks direct paleomagnetic constraints. Magnetic inclination data from the considerably older, underlying Dongjia Formation and from overlying Lower Cambrian strata indicate northern tropical latitudes (~5°N and 15°N, respectively; Huang et al., 1999; Zhang et al., 2000; Fu et al., 2015). The striated pavement of this study was developed on fine-grained sandstones of the Sanjiaotang Formation, which crop out along the eastern wall of a precipitous north-south–oriented valley at Shimengou, near Pingdingshan, Henan Province, China (Fig. 1).

METHODS

Multiple flights over the striated pavement at Shimengou were made using a DJI Mavic Pro unmanned aerial vehicle (UAV). From over 1000 aerial photographs taken at elevations ranging from 3 to 100 m, series of orthorectified models ("photographs") were produced from point cloud data in Agisoft Metashape (https://www.agisoft.com). The same point cloud data were used to produce digital elevation models (DEMs). The data were exported to QGIS (https://www.qgis.org/en/site/), layered with transparency algorithms, and combined to produce composite aerial images that show both photorealistic color and surface texture. The approach was supplemented by traditional outcrop description and outcrop photographs, which collectively served as the foundation for mapping. Although diamictite stratigraphically overlies the surface at a nearby road section (Fig. 1), sediment cover on the surface itself is extremely limited and cannot be demonstrated to be *in situ*. All data for the study are contained in this manuscript.

RESULTS

Description

The Shimengou pavement intermittently exposes a suite of subglacial bed forms over an ~1-km-long outcrop, on which three high-

quality exposure or study sites (Fig. 1) were identified. These study sites are referred to as the northern (Fig. 2), central (Fig. 3), and southern (Fig. 4) areas. At each site, we recognized a variety of plastically molded forms (or p-forms; Dahl, 1965), together with striations, the lateral

relationships of which were particularly clear in the northern site (Fig. 2). Following the classification of Kor et al. (1991), these included general faceted forms (Fig. 2, i), cavetto (Fig. 2, ii), classic müschelbruche (Fig. 2, iii), and spindle flutes (Fig. 2, iv). The p-forms are typically de-
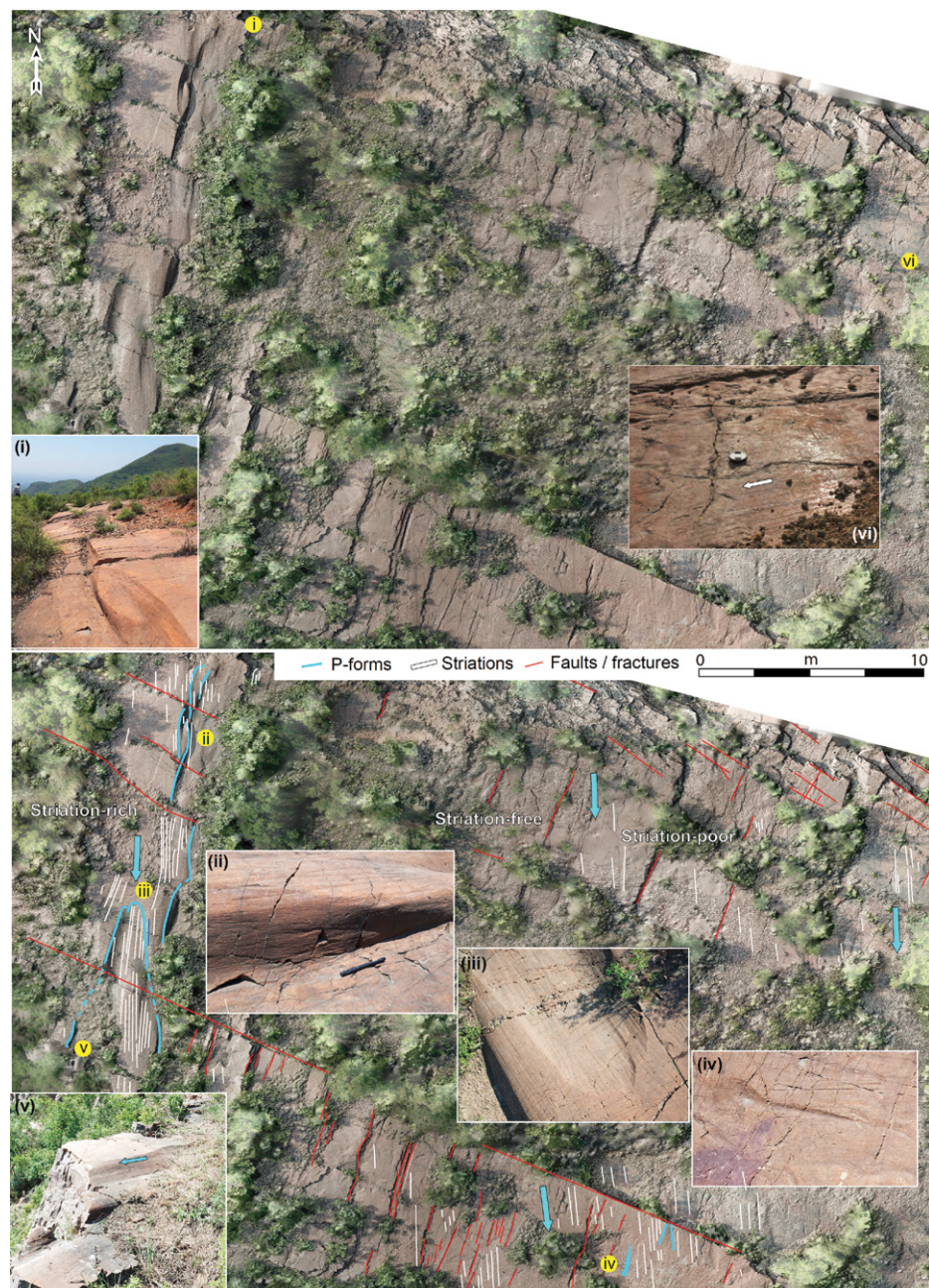

Figure 2. Composite aerial image of northern area of Shimengou outcrop, central China, with "clean" and "interpreted" images shown side-by-side. Inset photographs are located according to corresponding numbers. Exposure is traversed by classic p-forms and striations. Some of these crosscut earlier faults and fractures; others are themselves cut by later faults and fractures. Direction of ice flow, based on the geometry of p-forms, is indicated by arrow. Features shown in inset photos are as follows: (i) general view of p-forms and striations looking south, (ii) steep-sided cavetto, (iii) müschelbruche covered on all sides by striations, (iv) spindle flute, and (v) general view of steep-sided form at southern end of exposure. Note general division of exposure into striation-rich, striation-poor, and striation-absent domains. (vi) Photo illustrating a well-developed patina archiving two striation orientations crosscutting at 90°. Based on crosscutting relationships, initial (either east-west–, or west-east–directed) ice flow was followed by main (north-south) ice flow recorded everywhere else at Shimengou. Absence of this patina elsewhere appears to mask existence of this earlier ice-flow direction.
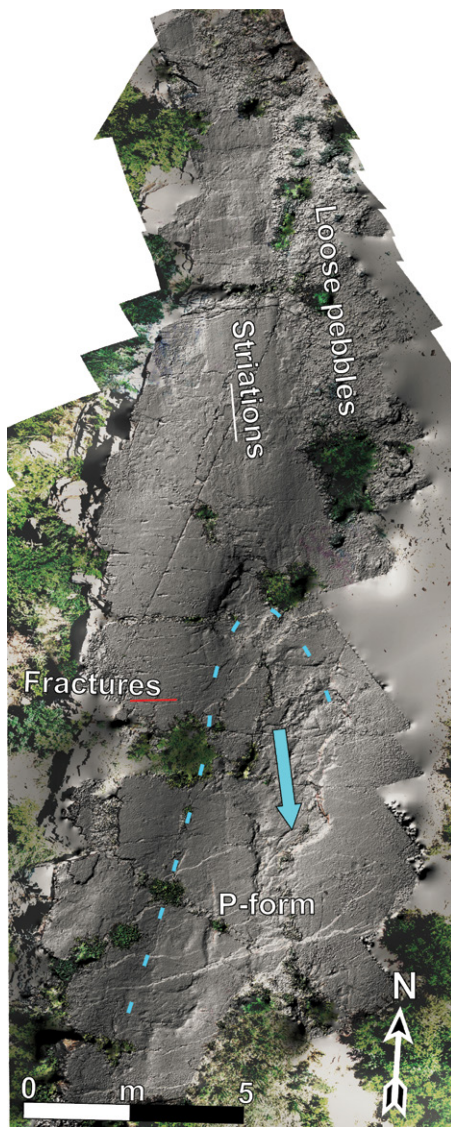
Figure 3. Composite aerial image from central area of Shimengou outcrop, central China. Note low-amplitude müschelbruche.
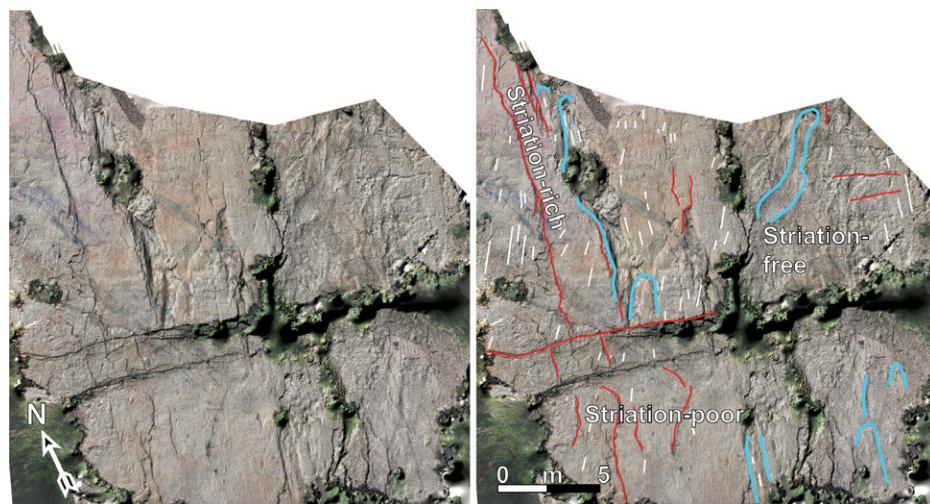

Figure 4. Composite aerial image from central area of Shimengou outcrop, central China. Note general division of exposure into striation-rich, striation-poor, and striation-absent domains.

fined by razor-sharp edges (Fig. 2, iii and iv). In some cases, glacial landforms cut preexisting faults and fractures, whereas in other cases, the reverse is true (Fig. 2).

At each study site (Fig. 1), the pavement exhibits local variations, most of which are only revealed by the composite aerial images. Significant lateral changes in the orientations of the p-forms and striations are apparent across the sandstone plateau. From north to south, these evolve from north-south to NNW-SSE to NNE-SSW trends. At the central study site (Fig. 1), the composite aerial image reveals striations together with very low-amplitude subglacial müschelbruche (amplitude of a few centimeters, wavelength of ~2 m; Fig. 3). At both the northern and southern sites (cf. Figs. 2 and 4), "striation-rich" areas transition into "striation-poor" or "striation-absent" areas. Rarely, the surface patina reveals a set of striations locally

oriented at 90° to the regional trend, i.e., east-west (Fig. 2, vi). In each of the three study sites, the pavement also exhibits transverse subparallel faults and fractures that are oriented approximately perpendicular to the glacial landforms. Some are intersected by the p-forms (Figs. 2C–2E), whereas in other cases, the p-forms are themselves crosscut by faults with a decimeter-scale throw (Fig. 3).

Interpretation

The collection of characteristic and well-established subglacial bed forms records the gradual abrasion of a lithified sandstone substrate beneath an ice mass in the presence of abundant subglacial meltwater. The unequivocal p-forms (Kor et al., 1991) testify to the genesis of these structures in the subglacial environment. This simple conclusion is important given that superficially similar striated surfaces in Neoproterozoic rocks—but lacking in striated p-forms—can be generated through gravitationally driven slope collapse in mountainous regions or in large underwater landslides (Draganits et al., 2008). The generation of the subglacial assemblage through tectonic uplift and faulting at the contact between the Sanjiaotang Formation and the Luoquan Formation is likewise discounted. The fractures and faults that cut the glacial bed forms developed both prior to and after the formation of the pavement, as indicated by the crosscutting relationships.

At Shimengou, the various structures were formed by abrasion but with substantial subglacial meltwater involvement. The range of structures present probably reflect high effective basal meltwater pressures (>1 MPa; Glasser and Bennett, 2004). These characteristics are compatible with the presence of temperate or polythermal glaciers (Hambrey and Glasser, 2012). The sharp "up-ice" morphology of the müschelbruche (Kor et al., 1991) allows a

general southward ice flow to be recognized (Figs. 2 and 3), and thus earlier suggestions of northward-flowing ice (Guan et al., 1986, their figure 1) are erroneous. The gradual changes in striation orientation from north to south across the plateau (cf. Figs. 1 and 2–4) indicate unidirectional yet slightly sinuous ice flow. These patterns were not recognized in previous work (Guan et al., 1986; Wu and Guan, 1988). The development of low-amplitude müschelbruche, some of which are apparent only on composite aerial imagery (Fig. 3), underscores the widespread lateral development of subglacial topography. Differentiation among striation-rich, striation-poor, or striation-absent areas may reflect subtle changes in substrate rheology, later meltwater removal, or recent differential weathering. While the latter certainly accounts for the absence of striations in some areas (Fig. 4), glaciological factors, such as meltwater distribution, are a more probable explanation in regions where a surface veneer survives yet striations are absent (Siman-Tov et al., 2017). Counter to this general picture, the evidence for local crosscutting striations, not revealed on the landscape-scale data set but only on a local patina (Fig. 2, vi), presents apparently conflicting information. These could be interpreted as locally complex ice flows (e.g., Rea et al., 2000), or more likely a previous east-west (or west-east) flow, the evidence for which was largely erased by the establishment of the north to south dominant flow.

DISCUSSION AND CONCLUSIONS

The data reveal (1) spatial variations in ice-flow direction that are generally south directed, (2) lateral variability in the density of striation development, (3) subtle undulose bed forms with amplitudes of a few centimeter, and (4) clear distinction of subglacial bed forms from earlier-formed and later-formed tectonic features. The

facts that striated pavements only occur beneath the Luoquan Formation, and no intraformational subglacial unconformities occur within the formation suggest that the fragmentary pavements from other areas of the North China block (Mu, 1981; Guan et al., 1986) probably formed during the same glacial cycle.

We interpret a well-lubricated ice-contact interface produced with substantial meltwater involvement. Significantly, these interpretations (1) provide rare evidence for subglacial process in rocks of this age, and (2) deliver a window into Ediacaran subglacial conditions. While the Shimengou pavement represents a glacial unconformity that is exceptional in terms of preservation in the Precambrian record, does it represent an exceptional glaciation? Ediacaran glaciations are increasingly viewed as nonglobal in nature, distinguishing them in style from the proposed snowball Earth events of the Cryogenian (Pu et al., 2016). Yet, the likely tropical latitude of the North China block (Li et al., 2013; Merdith et al., 2017) during the late Ediacaran makes an understanding of glacial dynamics particularly significant. The occurrence of ice-proximal diamictites over >2000 km of the Central China orogen (Le Heron et al., 2018) allows us to propose an ice margin of similar extent. This suggests a substantial ice cap in tropical latitudes. Even in the absence of posited snowball Earth conditions, this is remarkable.

How was such an outstanding pavement preserved? Based on the observation that closely spaced fracture sets promote enhanced glacial quarrying rates (Dühnforth et al., 2010), it could be speculated that the abundant fractures cross-cutting the pavement promoted the development of a local subglacial basin that was later buried by strata of the Luoquan Formation. At Shimengou, although substantial meltwater involvement in p-form generation is suspected, the absence of major later meltwater erosion features (e.g., scallops, chutes, potholes; Glasser and Nicholson, 1998) is notable. Abundant meltwater reworking would be expected during retreat of a major ice cap. The lack of evidence for this at Shimengou may point to distributed meltwater systems (Hewitt, 2011). The secret of outstanding preservation may lie, paradoxically, in the continental paleoenvironmental context and proposed glacilacustrine setting of the Luoquan Formation. If meltwater debouched into a lake system, the exposed subglacial unconformity would have been protected from the effects of surface (fluvial) erosion. Nevertheless, the entry of meltwater jet efflux into lakes is known to have an erosional effect (Carrivick and Tweed, 2013), suggesting that the Shimengou pavement may have lain between such entry points but protected by a preliminary sedimentary layer.

In the past 15 yr, major advances in understanding the flow behavior of deep-time ice masses have been made by combining traditional geologic fieldwork with the analysis of satellite image data (Moreau et al., 2005; Le Heron, 2018; Assine et al., 2018; Andrews et al., 2019). While UAV technology is widely applied at modern (Tonkin et al., 2016) ice margins, or in the study of Quaternary subglacial bed-form geomorphology (Ely et al., 2018; Chandler et al., 2018), it has never been used in the description of pre-Pleistocene glacial landforms, yet it provides a vital bridge in scale between outcrop and satellite image interpretation. Systematic mapping of Precambrian unconformities elsewhere should yield refined interpretations of the nature of deep-time masses, more objective comparison, and a fresh perspective. This perspective is greatly improved with a bird's-eye view of an ancient landscape.

REFERENCES CITED

Andrews, G.D., McGrady, A.T., Brown, S.R., and Maynard, S.M., 2019, First description of subglacial megalineations from the late Paleozoic ice age in southern Africa: PLoS One, v. 14, p. e0210673, https://doi.org/10.1371/journal.pone.0210673.

Assine, M.L., de Santa Ana, H., Veroslavsky, G., and Vesely, F.F., 2018, Exhumed subglacial landscape in Uruguay: Erosional landforms, depositional environments, and paleo–ice flow in the context of the late Paleozoic Gondwanan glaciation: Sedimentary Geology, v. 369, p. 1–12, https://doi.org/10.1016/j.sedgeo.2018.03.011.

Carrivick, J.L., and Tweed, F.S., 2013, Proglacial lakes: Character, behaviour and geological importance: Quaternary Science Reviews, v. 78, p. 34–52, https://doi.org/10.1016/j.quascirev.2013.07.028.

Carto, S.L., and Eyles, N., 2012, Sedimentology of the Neoproterozoic (c. 580 Ma) Squantum 'Tillite,' Boston Basin, USA: Mass flow deposition in a deep-water arc basin lacking direct glacial influence: Sedimentary Geology, v. 269–270, p. 1–14.

Chandler, B.M.P., et al., 2018, Glacial geomorphological mapping: A review of approaches and frameworks for best practice: Earth-Science Reviews, v. 185, p. 806–846, https://doi.org/10.1016/j.earscirev.2018.07.015.

Christie-Blick, N., 1982, Upper Precambrian (Eocambrian) Mineral Fork Tillite of Utah—A continental glacial and glaciomarine sequence: Discussion: Geological Society of America Bulletin, v. 93, p. 184–186, https://doi.org/10.1130/0016-7606(1982)93<184:UPEMFT>2.0.CO;2.

Corkeron, M., 2011, Neoproterozoic glacial deposits of the Kimberley Region and northwestern Northern Territory, Australia, in Arnaud, E., et al., eds., The Geological Record of Neoproterozoic Glaciations: Geological Society [London] Memoir 36, p. 659–672.

Corkeron, M.L., and George, A.D., 2001, Glacial incursion on a Neoproterozoic carbonate platform in the Kimberley region, Australia: Geological Society of America Bulletin, v. 113, p. 1121–1132, https://doi.org/10.1130/0016-7606(2001)113<1121:GIOANC>2.0.CO;2.

Crowell, J.C., 1964, Climate significance of sedimentary deposits containing dispersed megaclasts, in Nairn, A.E.M., ed., Problems in Palaeoclimatology: London, Interscience London, p. 86–99.

Dahl, R., 1965, Plastically sculptured detail forms on rock surfaces in northern Nordland, Norway: Geografiska Annaler, ser. A. Physical Geography, v. 47, p. 83, https://doi.org/10.1080/04353676.1965.11879716.

Daily, B., Gostin, V.A., and Nelson, C.A., 1973, Tectonic origin for an assumed glacial pavement of late Proterozoic age, South Australia: Journal of the Geological Society of Australia, v. 20, p. 75–78, https://doi.org/10.1080/14400957308527896.

Draganits, E., Schlaf, J., Grasemann, B., and Argles, T., 2008, Giant submarine landslide grooves in the Neoproterozoic/Lower Cambrian Phe Formation, northwest Himalaya: Mechanisms of formation and palaeogeographic implications: Sedimentary Geology, v. 205, p. 126–141, https://doi.org/10.1016/j.sedgeo.2008.02.004.

Dühnforth, M., Anderson, R.S., Ward, D., and Stock, G.M., 2010, Bedrock fracture control of glacial erosion processes and rates: Geology, v. 38, p. 423–426, https://doi.org/10.1130/G30576.1.

Ely, J.C., Graham, C., Barr, L.D., Rea, B.R., Spagnolo, M., and Evans, J., 2018, Using UAV acquired photography and structure from motion techniques for studying glacier landforms: Application to the glacial flutes of Isfallsglaciaren: Earth Surface Processes and Landforms, v. 42, p. 877–888, https://doi.org/10.1002/esp.4044.

Etemad-Saeed, N., Hosseini-Barzi, M., Adabi, M.H., Miller, N.R., Sadeghi, A., Houshmandzadeh, A., and Stockli, D.F., 2016, Evidence for ca. 560 Ma Ediacaran glaciation in the Kahar Formation, central Alborz Mountains, northern Iran: Gondwana Research, v. 31, p. 164–183, https://doi.org/10.1016/j.gr.2015.01.005.

Etienne, J.L., Allen, P.A., Le Guerroué, E., Heaman, L., Ghosh, S.K., and Islam, R., 2011, The Blaini Formation of the Lesser Himalaya, NW India, in Arnaud, E., et al., eds., The Geological Record of Neoproterozoic Glaciations: Geological Society, London, Memoirs, v. 36, p. 347–355, https://doi.org/10.1144/M36.31.

Fu, X., Zhang, S., Li, H., Ding, J., Li, H., Yang, T., Wu, H., Yuan, H., and Lv, J., 2015, New paleomagnetic results from the Huaibei Group and Neoproterozoic mafic sills in the North China craton and their paleogeographic implications: Precambrian Research, v. 269, p. 90–106, https://doi.org/10.1016/j.precamres.2015.08.013.

Glasser, N.F., and Bennett, M.R., 2004, Glacial erosional landforms: Origins and significance for palaeoglaciology: Progress in Physical Geography, v. 28, p. 43–75, https://doi.org/10.1191/0309133304pp401ra.

Glasser, N.F., and Nicholson, F.H., 1998, Subglacial meltwater erosion at Loch Treig: Scottish Journal of Geology, v. 34, p. 7–13, https://doi.org/10.1144/sjg34010007.

Guan, B.D., Wu, R.T., Hambrey, M.J., and Geng, W.C., 1986, Glacial sediments and erosional pavements near the Cambrian-Precambrian boundary in western Henan Province, China: Journal of the Geological Society, London, v. 143, p. 311–323, https://doi.org/10.1144/gsjgs.143.2.0311.

Hambrey, M.J., and Glasser, N.F., 2012, Discriminating glacier thermal and dynamic regimes in the sedimentary record: Sedimentary Geology, v. 251–252, p. 1–33, https://doi.org/10.1016/j.sedgeo.2012.01.008.

Hewitt, I.J., 2011, Modelling distributed and channelized subglacial drainage: The spacing of channels:

Journal of Glaciology, v. 57, p. 302–314, https://doi.org/10.3189/002214311796405951.

Huang, B., Yang, Z., Otofuji, Y., and Zhu, R., 1999, Early Paleozoic paleomagnetic poles from the western part of the North China block and their implications: Tectonophysics, v. 308, p. 377–402, https://doi.org/10.1016/S0040-1951(99)00098-0.

Iverson, N.R., 1991, Morphology of glacial striae: Implications for abrasion of glacier beds and fault surfaces: Geological Society of America Bulletin, v. 103, p. 1308–1316, https://doi.org/10.1130/0016-7606(1991)103<1308:MOGSIF>2.3.CO;2.

Jensen, P.A., and Wulff-Pedersen, E., 1996, Glacial or non-glacial origin for the Bigganjargga tillite, Finnmark, northern Norway: Geological Magazine, v. 133, p. 137–145, https://doi.org/10.1017/S0016756800008657.

Kor, P.S.G., Shaw, J., and Sharpe, D.R., 1991, Erosion of bedrock by subglacial meltwater, Georgian Bay, Ontario: A regional view: Canadian Journal of Earth Sciences, v. 28, p. 623–642, https://doi.org/10.1139/e91-054.

Krabbendam, M., Eyles, N., Putkinen, N., Bradwell, T., and Arbelaez-Moreno, L., 2016, Streamlined hard beds formed by palaeo–ice streams: A review: Sedimentary Geology, v. 338, p. 24–50, https://doi.org/10.1016/j.sedgeo.2015.12.007.

Laajoki, K., 2002, New evidence of glacial abrasion of the late Proterozoic unconformity around Varangerfjorden, northern Norway, in Altermann, W., and Corcoran, P.L., eds., Precambrian Sedimentary Environments: A Modern Approach to Ancient Depositional Systems: International Association of Sedimentologists Special Publication 33, p. 405–436.

Le Heron, D.P., 2018, An exhumed Paleozoic glacial landscape in Chad: Geology, v. 46, p. 91–94, https://doi.org/10.1130/G39510.1.

Le Heron, D.P., Vandyk, T.M., Wu, G., and Meng, Li., 2018, New perspectives on the Luoquan glaciation (Ediacaran-Cambrian) of North China: The Depositional Record, v. 4, p. 274–292, https://doi.org/10.1002/dep2.46.

Li, Z.X., Evans, D.A.D., and Halverson, G.P., 2013, Neoproterozoic glaciations in a revised global palaeogeography from the breakup of Rodinia to the assembly of Gondwanaland: Sedimentary Geology, v. 294, p. 219–232, https://doi.org/10.1016/j.sedgeo.2013.05.016.

Lu, S., and Gao, Z., 1994, Neoproterozoic tillite and tilloid in the Aksu area, Tarim Basin, Xinjiang Uygur Autonomous Region, Northwest China, in Deynoux, M., et al., eds., Earth's Glacial Record: Cambridge, UK, Cambridge University Press, p. 95–100.

Merdith, A.S., et al., 2017, A full-plate global reconstruction of the Neoproterozoic: Gondwana Research, v. 50, p. 84–134, https://doi.org/10.1016/j.gr.2017.04.001.

Mirams, R.C., 1964, A Sturtian glacial pavement at Merinjina Well, near Wooltana: Quarterly Geological Notes of the Geological Survey of South Australia, v. 11, p. 4–6.

Montes, A.S.L., Gravenor, C.P., and Montes, M.L., 1985, Glacial sedimentation in the late Precambrian Bebedouro formation, Bahia, Brazil: Sedimentary Geology, v. 44, p. 349–358, https://doi.org/10.1016/0037-0738(85)90019-3.

Moreau, J., Ghienne, J.-F., Le Heron, D.P., Deynoux, M., and Rubino, J.-L., 2005, A 440 million year old ice stream in North Africa: Geology, v. 33, p. 753–756, https://doi.org/10.1130/G21782.1.

Mu, Y., 1981, Luoquan Tillite of the Sinian System in China, in Hambrey, M.J., and Harland, W.B., eds., Earth's Pre-Pleistocene Glacial Record: Cambridge, UK, Cambridge University Press, p. 402–421.

Perry, W.J., and Roberts, H.G., 1968, Late Precambrian glaciated pavements in the Kimberley region, Western Australia: Journal of the Geological Society of Australia, v. 15, p. 51–56, https://doi.org/10.1080/00167616808728679.

Pu, J.P., Bowring, S.A., Ramezani, J., Myrow, P., Raub, T.D., Landing, E., Mills, A., Hodgin, E., and Macdonald, F.A., 2016, Dodging snowballs: Geochronology of the Gaskiers glaciation and the first appearance of the Ediacaran biota: Geology, v. 44, p. 955–958, https://doi.org/10.1130/G38284.1.

Rea, B.R., Evans, D.J.A., Dixon, T.S., and Whalley, W.B., 2000, Contemporaneous, localized, basal ice-flow variations: Implications for bedrock erosion and the origin of p-forms: Journal of Glaciology, v. 46, p. 470–476, https://doi.org/10.3189/172756500781833197.

Rice, A.H.N., and Hoffman, C.-C., 2000, Evidence for a glacial origin of Neoproterozoic III striations at Oaibaččannjar'ga, Finnmark, northern Norway: Geological Magazine, v. 137, p. 355–366, https://doi.org/10.1017/S0016756800004222.

Shen, B., Xiao, S., Dong, L., Zhou, C., and Liu, J., 2007, Problematic macrofossils from Ediacaran successions in the North China and Chaidam blocks: Implications for their evolutionary roots and biostratigraphic significance: Journal of Paleontology, v. 81, p. 1396–1411, https://doi.org/10.1666/06-016R.1.

Siman-Tov, S., Stock, G.M., Brodsky, E.E., and White, J.C., 2017, The coating layer of glacial polish: Geology, v. 45, p. 987–990, https://doi.org/10.1130/G39281.1.

Spence, G.H., Le Heron, D.P., and Fairchild, I.J., 2016, Sedimentological perspectives on climatic, atmospheric and environmental change in the Neoproterozoic Era: Sedimentology, v. 63, no. 2, p. 253–306, https://doi.org/10.1111/sed.12261.

Tonkin, T.N., Midgley, N.G., Cook, S.J., and Graham, D.J., 2016, Ice-cored moraine degradation mapped and quantified using an unmanned aerial vehicle: A case study from a polythermal glacier in Svalbard: Geomorphology, v. 258, p. 1–10, https://doi.org/10.1016/j.geomorph.2015.12.019.

Wu, R.T., and Guan, B.D., 1988, Glacigenic characteristics of the Luoquan Formation and sediment gravity flow reworking on it: Acta Geologica Sinica, v. 1, p. 325–339 [in Chinese with English abstract].

Zhang, S., Li, Z.-X., Wu, H., and Wang, H., 2000, New paleomagnetic results from the Neoproterozoic successions in southern North China block and paleogeographic implications: Science in China, ser. D, Earth Sciences, v. 43, p. 233–244, https://doi.org/10.1007/BF02911948.

Zhou, C., Yuan, X., Xiao, S., Chen, Z., and Hua, H., 2018, Ediacaran integrative stratigraphy and timescale of China: Science in China, ser. D, Earth Sciences, v. 62, p. 7–24, https://doi.org/10.1007/s11430-017-9216-2.

Printed in USA